J. Biochem. 2012;152(3):231–239 doi:10.1093/jb/mvs064

JB THE JOURNAL OF BIOCHEMISTRY

Effects of site-directed mutagenesis of Asn116 in the β-hairpin of the N-terminal domain of thermolysin on its activity and stability

Received April 3, 2012; accepted May 7, 2012; published online May 29, 2012

Evans Menach, Kiyoshi Yasukawa and Kuniyo Inouye*

Division of Food Science and Biotechnology, Graduate School of Agriculture, Kyoto University, Sakyo-ku, Kyoto 606-8502, Japan

*Kuniyo Inouye, Division of Food Science and Biotechnology, Graduate School of Agriculture, Kyoto University, Sakyo-ku, Kyoto 606-8502, Japan. Tel: +81-75-753-6266, Fax: +81-75-753-6265, email: inouye@kais.kyoto-u.ac.jp

In the N-terminal domain of thermolysin, two anti-parallel β-strands, Asn112–Ala113–Phe114–Trp115 and Ser118–Gln119–Met120–Val121–Tyr122 are connected by an Asn116–Gly117 turn to form a β-hairpin structure. In this study, we examined the role of Asn116 in the activity and stability of thermolysin by site-directed mutagenesis. Of the 19 Asn116 variants, four (N116A, N116D, N116T and N116Q) were produced in *Escherichia coli*, by co-expressing the mature and pro domains separately, while the other 15 were not. In the hydrolysis of *N*-[3-(2-furyl)acryloyl]-glycyl-L-leucine amide (FAGLA) at 25°C, the intrinsic k_{cat}/K_m value of N116D was 320% of that of the wild-type thermolysin (WT), and in the hydrolysis of *N*-carbobenzoxy-L-aspartyl-L-phenylalanine methyl ester (ZDFM) at pH 7.5 at 25°C, the k_{cat}/K_m value of N116D was 140% of that of WT, indicating that N116D exhibited higher activity than WT. N116Q exhibited similar activity as WT, and N116A and N116T exhibited reduced activities. The first-order rate constants, k_{obs}, of the thermal inactivation at 80°C were in the order N116A, N116D, N116T > N116Q > WT at all $CaCl_2$ concentrations examined (1–100 mM), indicating that all variants exhibited reduced stabilities. These results suggest that Asn116 plays an important role in the activity and stability of thermolysin presumably by stabilizing this β-hairpin structure.

Keywords: β-hairpin/metalloproteinase/site-directed mutagenesis/stability/thermolysin.

Abbreviations: FAGLA, *N*-[3-(2-furyl)acryloyl]-glycyl-L-leucine amide; ZDFM, *N*-carbobenzoxy-L-aspartyl-L-phenylalanine methyl ester.

Thermolysin [EC 3.4.24.27] is a thermostable neutral metalloproteinase that belongs to Gluzincins and subclan MA(E) in clan MA. It was originally identified in the culture broth of *Bacillus thermoproteolyticus* (*1–3*). It requires one zinc ion essential for enzyme activity and four calcium ions for structural stability (*4–6*). It consists of 316 amino acid residues with a β-rich N-terminal domain (Ile1–Asp138) and an α-helical C-terminal domain (Asp150–Lys316). These two domains are connected by an α-helix (Val139–Thr149) located at the bottom of the active site cleft (Fig. 1A) (*7*). It specifically catalyses the hydrolysis of peptide bonds containing hydrophobic amino acid residues (*8*, *9*). It is used in industry for peptide bond formation through reverse reaction of hydrolysis. The most extensive use is in the synthesis of *N*-carbobenzoxy-L-aspartyl-L-phenylalanine methyl ester (ZDFM) from *N*-carbobenzoxy-L-aspartic acid (ZD) and L-phenylalanine methyl ester (FM) (*10*, *11*). ZDFM is a precursor of an artificial sweetener aspartame, which is 200 times sweeter than sucrose. Hence the improvement of its activity and stability are important subjects.

The active site of thermolysin comprises one zinc ion and five polypeptide regions, which are N-terminal sheet (Asn112–Trp115), α-helix 1 (Val139–Thr149), C-terminal loop 1 (Asp150–Gly162), α-helix 2 (Ala163–Val176) and C-terminal loop 2 (Gln225–Ser234). Previously we introduced single amino-acid substitutions into each of the 12 residues (Ala113, Phe114, Trp115, Asp150, Tyr157, Gly162, Ile168, Ser169, Asp170, Asn227, Val230 and Ser234) in these regions by site-directed mutagenesis and examined their effects on activity and stability (*12*). The results revealed that the N-terminal sheet and the α-helix 2 are critical in catalysis and the C-terminal loops 1 and 2 are important in substrate recognition (*12*). In that study, we found that two variants (D150E and I168A) were more active than the wild-type thermolysin (WT), and that seven variants (D150H, D150W, I168A, I168H, N227A, N227H and S234A) were more stable than WT (*12*). (In this study, the mutation of a residue for example Asp150 to Glu was designated as Asp150→Glu, and the thermolysin variant bearing the mutation was designated as D150E).

In the N-terminal domain of thermolysin, two anti-parallel β-strands (Asn112–Ala113–Phe114–Trp115 and Ser118–Gln119–Met120–Val121–Tyr122) are connected by an Asn116–Gly117 turn to form a β-hairpin structure (Fig. 1B and C). The Asn112–Trp115 strand is located in the active site and forms the S2′, S1′ and S2 subsites, while the Ser118–Tyr122 strand and the Asn116–Gly117 turn are located outside the active site (*9*). [The subsites and the corresponding residues in the substrates are designated based upon the nomenclature of

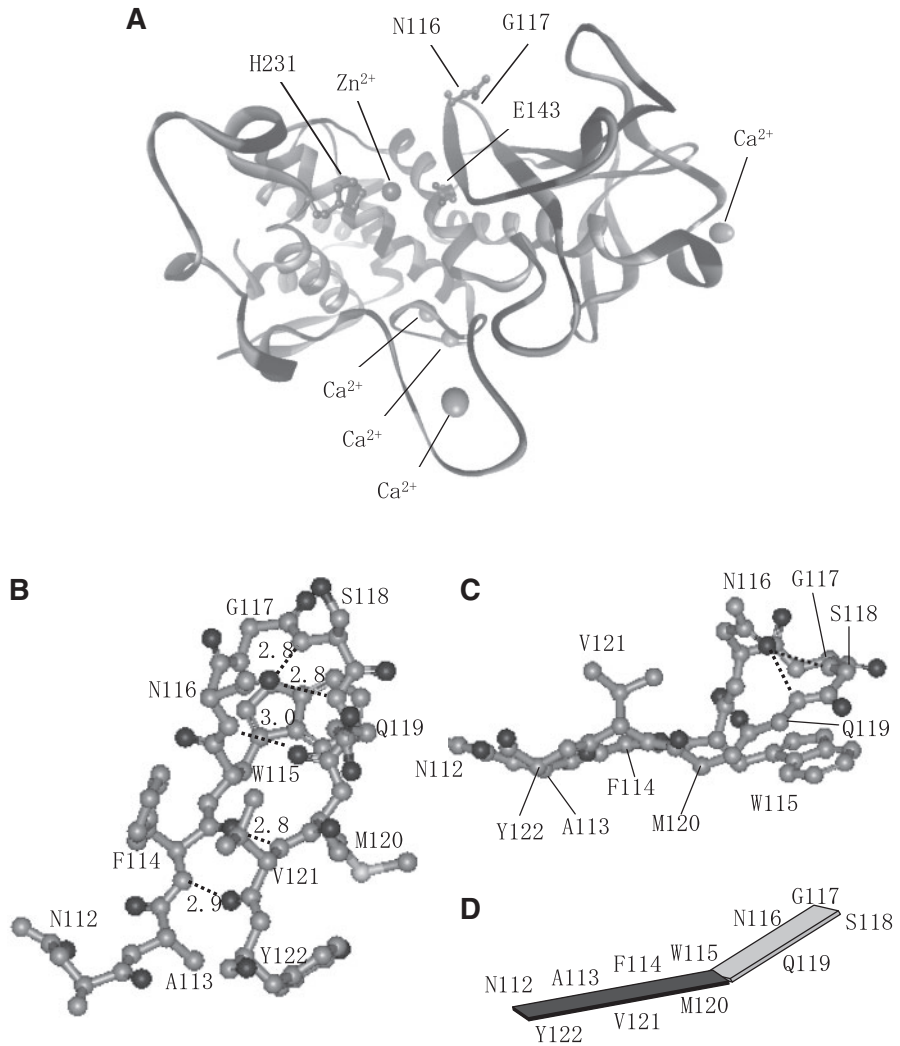

Fig. 1 Structure of thermolysin. The structure is based on Protein Data Bank accession number 8TLN. (A) Overall protein structure. The main chain is represented by a ribbon model. Side chains of Asn116 and Gly117 and the catalytically important residues Glu143 and His231 are represented by a ball and stick. Zinc and calcium ions are shown as spheres. (B and C) Close-up view of the Asn112–Trp115 strand, the Asn116–Gly117 loop and the Ser118–Tyr122 strand. All atoms are shown by a ball and stick (B), and all main-chain atoms and the side-chain atoms of Trp115, Asn116 and Val121 are shown by a ball and stick (C). Oxygen is coloured black, and carbon, nitrogen, and sulphur gray. Hydrogen bonds are represented by dotted lines together with the distances (Å). (D) Illustration of the two β-planes formed by Asn112–Trp115 and Met120–Tyr122 and by Trp115–Met120.

Schechter, I. and Berger, A. (*13*)]. Previously we reported that G117E had higher activity in the hydrolysis of ZDFM but lower activity in the hydrolysis of *N*-[3-(2-furyl)acryloyl]-glycyl-L-leucine amide (FAGLA) than WT, suggesting that Gly117 plays an important role in substrate specificity (*14*). In this study, to explore the catalytic role of this β-hairpin structure and possibly produce a variant enzyme with high performance, we introduced 19 amino-acid substitutions into Asn116 by site-directed mutagenesis and examined their effects on activity and stability.

Materials and Methods

Materials

Bovine milk casein of Hammerstein grade (lot no. WKL1761) was purchased from Wako Pure Chemical (Osaka, Japan). FAGLA (lot no. 111K1764) was purchased from Sigma (St. Louis, MO). The concentration of FAGLA and ZDFM were determined spectrophotometrically using the molar absorption co-efficient, $\varepsilon_{345} = 766\,M^{-1}cm^{-1}$ (*10*) and $\varepsilon_{257} = 387\,M^{-1}cm^{-1}$(*10*) respectively.

Expression and purification of thermolysin

Expression in *E. coli* (*15*) and purification of recombinant thermolyin (*15*, *16*) were carried out as described previously. Briefly, the mature sequence of thermolysin containing the pelB leader sequence at its N-terminus and the pre-prosequence of thermolysin was expressed in JM109 cells. The mature thermolysin was purified to homogeneity from the supernatants of *E. coli* cultures by hydrophobic-interaction chromatography followed by affinity chromatography. The concentration was determined spectrophotometrically using an absorbance value at 277 nm (1 mg/ml) of 1.83 and a molecular mass of 34.6 kDa (*10*). Site-directed mutagenesis was carried out using Quikchange™ site-directed mutagenesis kit (Stratagene, La Jolla, CA, USA) for construction of Asn116 variants.

SDS–PAGE

Escherichia coli supernatants and purified thermolysin were analysed by SDS–PAGE with 12.5% polyacrylamide gel under reducing conditions according to the method of Laemmli (*17*). Samples were

reduced by treatment with 2.5% 2-mercaptoethanol at 100°C for 10 min and were applied to the gel. The molecular marker kit (Takara Bio, Otsu, Japan) consisting of rabbit muscle phosphorylase *b* (97.4 kDa), bovine serum albumin (66.3 kDa), rabbit muscle aldolase (42.4 kDa), bovine erythrocyte carbonic anhydrase (30.0 kDa), soybean trypsin inhibitor (20.1 kDa) and hen egg white lysozyme (14.4 kDa) was also applied. After the electrophoresis with a constant current of 40 mA for 40 min, proteins were stained with Coomassie Brilliant Blue R-250.

CD measurement

The CD spectra were measured using 2-mm cell with Jasco J-820 (Tokyo, Japan) spectropolarimeter equipped with a Peltier system of cell temperature control. Ellipticity was reported as mean residue molar ellipticity [θ] (deg cm^2 dmol^{-1}). The spectrometer conditions were: spectral range 200–260 nm; 100 mdeg sensitivity; 0.1-nm resolutions; 4 s response time; 20 nm min^{-1} scan rate; and seven accumulations. The control baseline was obtained with solvent and all the components without the proteins.

Hydrolysis of casein, FAGLA and ZDFM

The casein-, FAGLA- and ZDFM-hydrolysing activities of thermolysin were measured according to the methods described previously (*3*, *10*, *14*). In the casein-hydrolysing activity, the absorbance at 275 nm (A_{275}) of the acid-soluble fraction of the reaction solution was measured. One proteolytic unit (PU) is defined as the amount which liberates a quantity of acid-soluble peptides that corresponds to an increase in A_{275} of 0.0074 (A_{275} of 1 μg of tyrosine)/min (*3*).

In the FAGLA-hydrolysing activity, the decrease in A_{345} of the reaction solution was measured. The amount of FAGLA hydrolysed was evaluated using the molar absorption difference due to hydrolysis, $\Delta\varepsilon_{345} = -310\ \mathrm{M^{-1}cm^{-1}}$, at 25°C (*10*, *18*). The specificity constant (k_{cat}/K_m) was determined based on the Michaelis–Menten equation. The intrinsic k_{cat}/K_m ($(k_{cat}/K_m)_o$) and the proton dissociation constants at the acidic and alkaline sides (K_{e1} and K_{e2}, respectively) of the bell-shaped pH-dependence of the activity (k_{cat}/K_m) were calculated from Equation (1).

$$(k_{cat}/K_m)_{obs} = (k_{cat}/K_m)_o / \{1 + ([H]/K_{e1}) + (K_{e2}/[H])\} \quad (1)$$

In the ZDFM-hydrolysing activity, the decrease in A_{224} of the reaction solution was measured. The amount of ZDFM hydrolysed was evaluated using the molar absorption difference due to hydrolysis, $\Delta\varepsilon_{224} = -493\ \mathrm{M^{-1}cm^{-1}}$, at 25°C (*10*). The k_{cat} and K_m values of thermolysin were separately determined with Kaleida Graph Version 4.0 (Hulinks, Tokyo, Japan), based on the Michaelis–Menten equation by the non-linear least-squares method.

Thermal inactivation of thermolysin

Thermal inactivation of thermolysin were measured according to the methods described previously (*14*). Briefly, thermolysin was incubated at 80°C in the presence of 1–100 mM $CaCl_2$ for a specified duration, and the remaining activity to hydrolyse FAGLA was determined as described above. The first-order rate constant (k_{obs}) of the thermal inactivation was calculated by plotting the natural logarithm of the remaining activity (k_{cat}/K_m) against the time of thermal treatment.

Results

Production of Asn116 variants to homogeneity

Asn116 was changed into either one of the 19 amino acids. The WT and the variants were expressed in *E. coli* in the system (*15*), in which the mature and pro domains were expressed as independent polypeptides. Figure 2 shows a time-course for a flask-shake culture of the transformants. In all transformants, the OD_{600} of the cultures increased with an increase in time and reached the maximum (~3.0 for the transformant with pUC19 and 1.2–2.3 for the transformants with the expression plasmids for thermolysin) after 18 or 24 h (Fig. 2A). After the aforementioned duration, in WT, N116A, N116D, N116T and N116Q, the OD_{600} decreased with an increase in time, while in the other 15 variants, it was almost stable. In WT, N116A, N116D, N116T and N116Q, casein hydrolysis activity appeared in the supernatant and increased progressively even after OD_{600} reached the maximum level, while in the other 15 variants, it did not appear (Fig. 2B).

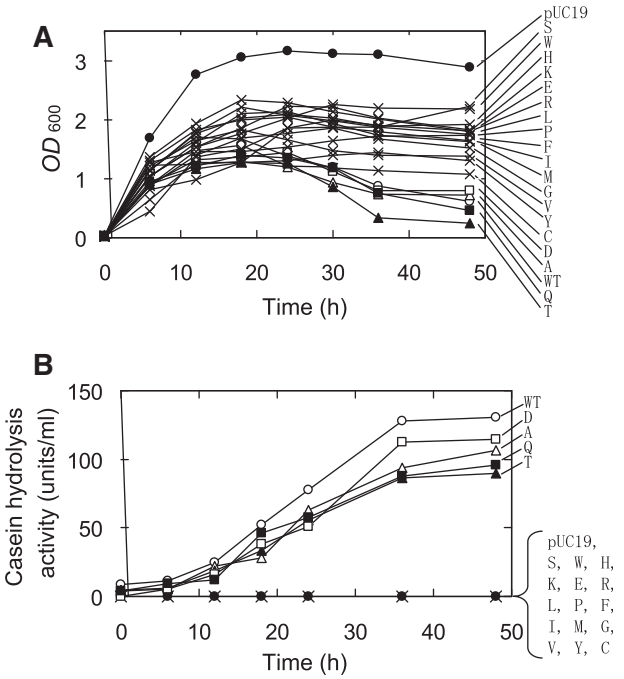

Fig. 2 Fermentation of *E. coli*. (A) Cell densities. (B) Casein hydrolysis activities. OD_{600} of culture (A) and casein hydrolysis activities of the supernatants (B) of *E. coli* cells transformed with pUC19 (filled circle) or the expression plasmids for WT (unfilled circle), N116A (unfilled triangle), N116D (unfilled square), N116T (filled triangle), N116Q, (filled square), or the other 15 variants (+) are plotted against time. 0 h means start of flask-shake culture. Variant names are abbreviated: for example, 'A' indicates N116A.

Figure 3A and B show the SDS–PAGE of the culture supernatants of the *E. coli* cells transformed with the expression plasmids for WT and the variants. The 34-kDa protein band was clearly detected for WT, N116A, N116D, N116T and N116Q, but was not for the other 15 variants. Figure 3C shows the SDS–PAGE of the purified preparation of WT, N116A, N116D, N116T and N116Q. They yielded a single band with a molecular mass of 34 kDa. Table 1 shows the representative purification data of WT and the four variants. From 450–480 ml of culture supernatants, 0.9–1.6 mg of purified enzymes were obtained. The specific activities of N116A, N116D, N116T and N116Q in the hydrolysis of casein at 25°C were 44, 66, 45 and 57%, respectively, of that of WT. Figure 3D shows the CD spectra of the purified enzymes at 200–260 nm. Each spectrum was characterized by negative ellipticities at ~202–240 nm with the peaks ~208 and 225 nm, suggesting that no significant conformational change was occasioned in thermolysin by the mutations.

Activity of Asn116 variants

Figure 4A shows the pH-dependence of k_{cat}/K_m of the thermolysin-catalysed hydrolysis of FAGLA at 25°C.

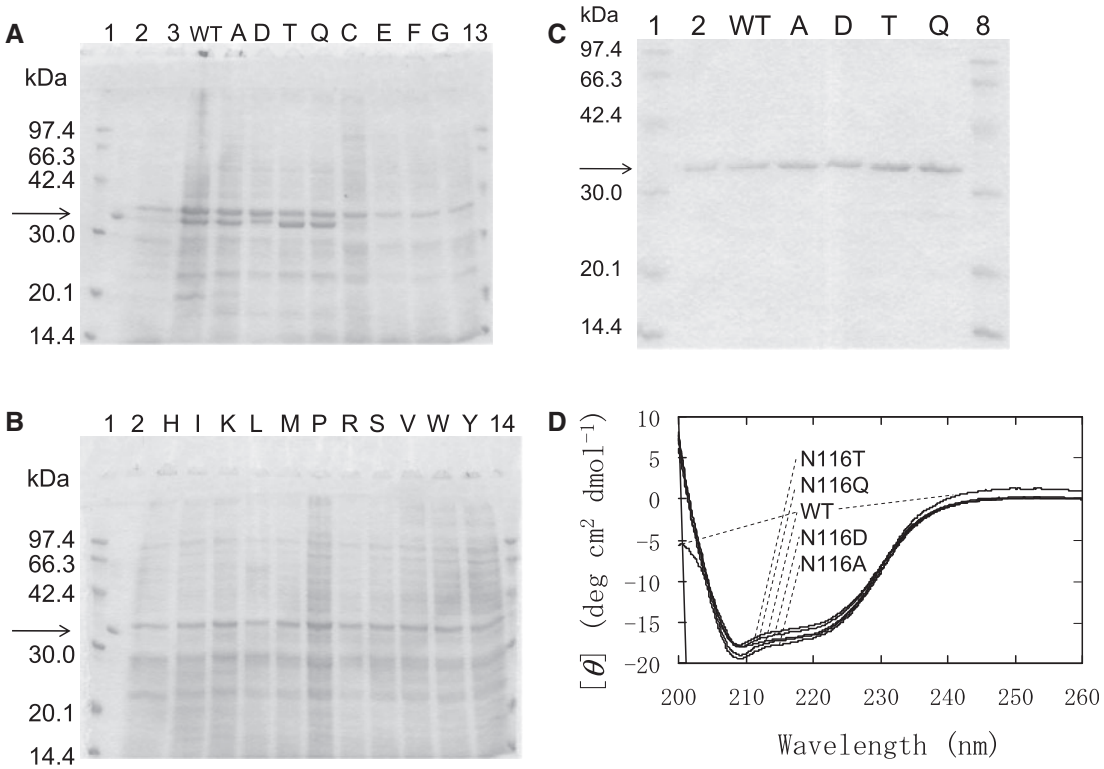

Fig. 3 Expression and purification of Asn116 variants. (A–C) Coomassie brilliant blue-stained 12.5% SDS–PAGE gels. (A) The marker proteins (lanes 1 and 13), native thermolysin purified from *B. thermoproteolyticus* (lane 2), and the supernatants of *E. coli* cells transformed with pUC-19 (lane 3) and the expression plasmids for WT (lane WT), N116A (lane A), N116D (lane D), N116T (lane T), N116Q (lane Q), N116C (lane C), N116E (lane E), N116F (lane F), N116G (lane G); (B) The marker proteins (lanes 1 and 14), native thermolysin purified from *B. thermoproteolyticus* (lane 2), and the supernatants of *E. coli* cells transformed with the expression plasmids for N116H (lane H), N116I (lane I), and N116K (lane K), N116L (lane L), N116M (lane M), N116P (lane P), N116R (lane R), N116S (lane S), N116V (lane V), N116W (lane W), and N116Y (lane Y); (C) The marker proteins (lanes 1 and 8), native thermolysin purified from *B. thermoproteolyticus* (lane 2), and purified preparations of WT (lane WT), N116A (lane A), N116D (lane D), N116T (lane T), and N116Q (lane Q). The arrow indicates the band corresponding to thermolysin. (D) CD spectra. CD spectra were measured for 2.1 μM thermolysin in 5 mM Tris–HCl, 10 mM $CaCl_2$ at pH 7.5, at 25°C.

Table I. Representative purification of Asn116 variants from the supernatant of the *E. coli* transformants.

	Volume (ml)	Activity (units)	Recovery (%)	Protein (mg)	Specific activity (units/mg)	Purification (fold)
WT						
Culture supernatant	450	59,000	100	54	1,100	1.0
Phenyl chromatography	180	34,000	58	8.8	3,800	3.4
Affinity chromatography	7.8	11,000	19	0.9	12,000	11
N116A						
Culture supernatant	480	51,000	100	67	760	1.0
Phenyl chromatography	150	21,000	41	12	1,800	2.3
Affinity chromatography	9.1	8,500	17	1.6	5,300	7.0
N116D						
Culture supernatant	480	54,000	100	68	790	1.0
Phenyl chromatography	180	27,000	50	13	2,100	2.7
Affinity chromatography	11	11,000	20	1.4	7,900	10
N116T						
Culture supernatant	460	41,000	100	74	550	1.0
Phenyl chromatography	170	21,000	51	13	1,600	2.9
Affinity chromatography	10	8,600	21	1.6	5,400	9.8
N116Q						
Culture supernatant	480	46,000	100	49	940	1.0
Phenyl chromatography	180	30,000	65	14	2,100	2.2
Affinity chromatography	7.5	6,800	15	1.0	6,800	7.2

All plots showed bell-shaped curves with the optimal pH of 6–7. The results are summarized in Table 2. The pK_{e1}, pK_{e2} and $(k_{cat}/K_m)_o$ values of WT (5.1 ± 0.2, 8.2 ± 0.1, $37 \pm 3\,mM^{-1}\,s^{-1}$, respectively) are almost the same as the ones we previously reported (5.3 ± 0.0, 8.3 ± 0.0 and $40 \pm 1\,mM^{-1}\,s^{-1}$, respectively) (*12*). The $(k_{cat}/K_m)_o$ values of N116D was 320% of that of WT, and those of the other three variants were

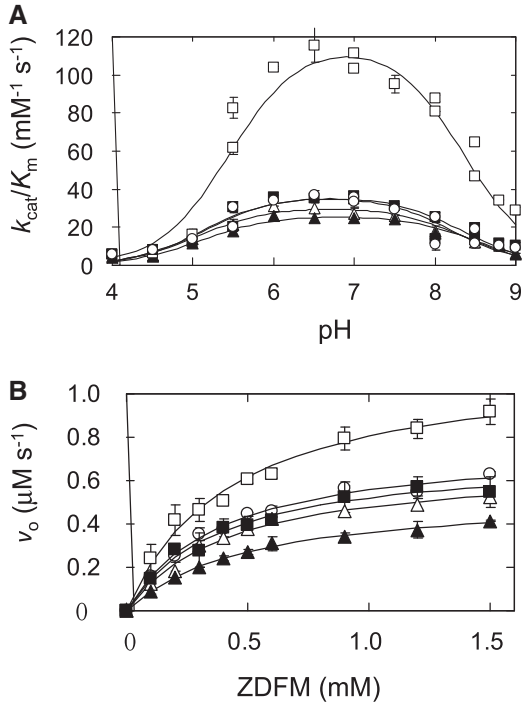

Fig. 4 Activity of Asn116 variants. (A) Effect of pH on the initial reaction rate (v_o) in the hydrolysis of FAGLA. The reaction was carried out in 40 mM acetate–NaOH at pH 4.0–5.5, 40 mM MES–NaOH at pH 5.5–7.0, 40 mM HEPES–NaOH at pH 7.0–8.5, and 40 mM TAPS–NaOH at pH 8.0–9.0, each of which contained 10 mM $CaCl_2$, at 25°C. The initial concentrations of enzyme and FAGLA were 100 nM and 400 μM, respectively. (B) Dependence of v_o on substrate concentration in the hydrolysis of ZDFM. The reaction was carried out in 40 mM Tris–HCl, 10 mM $CaCl_2$ at pH 7.5, at 25°C. Symbols for enzymes: WT, unfilled circle; N116A, unfilled triangle; N116D, unfilled square; N116T, filled triangle; N116Q, filled square. Error bars indicate SD values for three-times measurements.

Table II. pK_e values and intrinsic k_{cat}/K_m ($(k_{cat}/K_m)_o$) of Asn116 variants in the hydrolysis of FAGLA at 25°C.

Thermolysin	pK_{e1}	pK_{e2}	$(k_{cat}/K_m)_o$ (mM^{-1}s^{-1})
WT	5.1 ± 0.2 (0.0)	8.2 ± 0.1 (0.0)	37 ± 3 (1.0)
N116A	5.1 ± 0.1 (±0.0)	8.3 ± 0.1 (+0.1)	31 ± 1 (0.8)
N116D	5.4 ± 0.1 (+0.3)	8.4 ± 0.1 (+0.2)	117 ± 6 (3.2)
N116T	5.1 ± 0.1 (±0.0)	8.5 ± 0.1 (+0.3)	26 ± 1 (0.7)
N116Q	5.1 ± 0.2 (±0.0)	8.3 ± 0.1 (+0.1)	37 ± 3 (1.0)

Average of triplicate determinations with SD values is shown. Numbers in parentheses indicate ΔpK_e compared to the WT and the $(k_{cat}/K_m)_o$ relative to WT.

70–100% of that of WT. The pK_{e1} and pK_{e2} values of the variants were almost the same as those of WT.

Thermolysin activity increases with the increase in concentration of neutral salts (*10*). We defined the degree of the activation as the ratio of the k_{cat}/K_m value with 4 M NaCl to that without NaCl, and showed that it is in the range of 13–15 in the hydrolysis of FAGLA (*3*, *9*, *10*). The k_{cat}/K_m values at pH 7.5 without NaCl and with 4 M NaCl and the degree of the activation were 30 ± 4 mM^{-1} s^{-1}, 440 ± 29 mM^{-1} s^{-1} and 15 for WT, 24 ± 3 mM^{-1} s^{-1}, 330 ± 30 mM^{-1} s^{-1} and 14 for N116A, 95 ± 4 mM^{-} s^{-1}, 1000 ± 100 mM^{-1} s^{-1} and 11 for N116D, 24 ± 1 mM^{-1} s^{-1}, 240 ± 10 mM^{-1} s^{-1} and 10 for N116T, 31 ± 3 mM^{-1} s^{-1}, 270 ± 40 mM^{-1} s^{-1} and 9 for N116Q. Thus, the degrees of the NaCl-induced activation of the variants were 60–90% of that of WT.

Figure 4B shows the dependence of the initial reaction rate (v_o) of the thermolysin-catalysed hydrolysis of ZDFM on the substrate concentration at pH 7.5, at 25°C. All plots showed saturated profiles. The kinetic parameters are summarized in Table 3. The K_m values of the variants were 100–130% of that of WT. The k_{cat} value of N116D was 160% of that of WT, and those of the other three variants were 70–92%. Accordingly, the k_{cat}/K_m value of N116D was 140% of that of WT, and those of other three variants were 60–100%. These results indicate that N116D has higher activity than WT. They also indicate that N116Q has similar activity as WT, and N116A and N116T have reduced activities.

Stability of Asn116 variants

We examined time-dependences of the thermal inactivation of WT and the variants at 80°C in the presence of various concentrations of $CaCl_2$ ranging 1–100 mM. All inactivations followed pseudo-first-order kinetics (Fig. 5A for 10 mM $CaCl_2$, data not shown for 1, 30, 50 and 100 mM $CaCl_2$). Figure 5B shows the first-order rate constants, k_{obs}, of thermal inactivation of WT and the variants at each $CaCl_2$ concentration. They decreased with increasing $CaCl_2$ concentrations and were in the order N116A, N116D, N116T > N116Q > WT at all $CaCl_2$ concentrations examined.

Discussion

Catalytic role of Asn116

Figure 6A shows the typical β-hairpin peptide backbone with two amino acid residues (t1 and t2) at the turn (*19*). The most common t1 and t2 residues are Asn and Gly, respectively, followed by Gly and Ser. Thus not only Asn116 and Gly117 but also Gly117 and Ser118 can be ascribed to t1 and t2 residues, respectively. Figure 1B is a close-up view of the polypeptide Asn112–Tyr122, in which side chains of all residues are shown. It appears that side chains of Trp115, Asn116 and Val121 are located inside the β-plane formed by the Asn112–Trp115 and Ser118–Tyr122 β-strands, while those of other residues are located outside it. The carbonyl oxygen (OD1) of Asn116 is involved in two hydrogen bonds, one with the main-chain nitrogen (N) of Ser118 and the other with N of Gln119. Such hydrogen bonds are absent in the typical β-hairpin peptide backbone (Fig. 6A). Figure 1C is another close-up view of the polypeptide Asn112–Tyr122, in which side chains of Trp115, Asn116 and Val121 are shown. It appears that there are two β-planes, one formed by the polypeptides Asn112–Trp115 and Met120–Tyr122 and the other formed by Trp115–Met120. The side chain of Asn116 is located in the β-plane formed by

Table III. Kinetic parameters of Asn116 variants in the hydrolysis of ZDFM at 25°C.

Thermolysin	K_m (mM)	k_{cat} (s^{-1})	k_{cat}/K_m (mM^{-1} s^{-1})
WT	0.39 ± 0.04 (1.0)	7.7 ± 0.1 (1.0)	20 ± 1 (1.0)
N116A	0.41 ± 0.04 (1.1)	6.7 ± 0.7 (0.8)	16 ± 1 (0.8)
N116D	0.43 ± 0.04 (1.1)	12 ± 1 (1.5)	27 ± 2 (1.4)
N116T	0.49 ± 0.03 (1.3)	5.4 ± 0.1 (0.7)	11 ± 1 (0.6)
N116Q	0.38 ± 0.06 (1.0)	7.1 ± 0.1 (0.9)	19 ± 1 (1.0)

Average of triplicate determinations with SD value is shown. Numbers in parentheses indicate values relative to the WT.

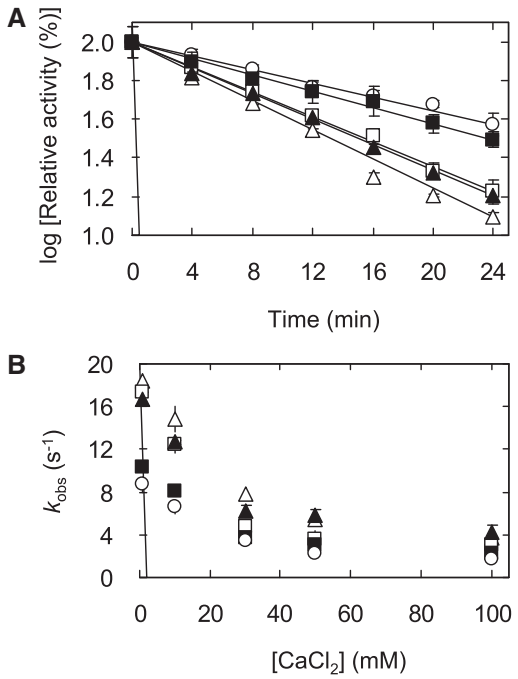

Fig. 5 Thermal stability of Asn116 variants. (A) Thermal inactivation at 10 mM $CaCl_2$. (**B**) Effect of $CaCl_2$ concentration on the thermal inactivation. Thermolysin (2 μM) in 40 mM HEPES–NaOH, 1, 10, 30, 50 or 100 mM $CaCl_2$ at pH 7.5 was incubated at 80°C for a specified duration. The FAGLA-hydrolytic reaction was carried out at 25°C with the initial concentrations of enzyme and FAGLA of 100 nM and 400 μM, respectively. The remaining activity (k_{cat}/K_m) was expressed as the relative value to that of the intact enzyme (WT, 29 mM^{-1} s^{-1}; N116A, 23 mM^{-1} s^{-1}; N116D, 95 mM^{-1} s^{-1}; N116T, 23 mM^{-1} s^{-1}; and N116Q, 29 mM^{-1} s^{-1}) and plotted against the incubation time (A). The first-order rate constants, k_{obs}, of thermal inactivation of thermolysin were plotted against the $CaCl_2$ concentration (B). Symbols correspond to those of Fig. 4. Error bars indicate SD values for three-times measurements.

Trp115–Met120, while those of Trp115 and Val121 are outside of these two β-planes. This is in contrast to the recent reports that the Trp–Trp interaction between the two β strands is important for the stability of β-hairpin structure (*20–22*). Figure 1D shows the illustration of the two β-plane structure formed by the polypeptide Asn112–Tyr122. Such structure is absent in the typical β-hairpin peptide backbone (Fig. 6A).

In this study, we used the *E. coli* expression system which does not require autocatalytic cleavage: the mature domain and the pre-prodomain of thermolysin were co-expressed constitutively as independent polypeptides under the original promoter sequences in the *npr* gene, which encodes thermolysin (*15*). Previously we reported that all 70 variants, in which 1 of 12 active-site residues (Ala113, Phe114, Trp115, Asp150, Tyr157, Gly162, Ile168, Ser169, Asp170, Asn227, Val230 and Ser234) was replaced into either of Asp, Glu, His, Lys, Arg, or Ala, could be produced at similar levels by this expression system whether they retained activity or not (*12*). In this study, of the 19 Asn116 variants, only four were produced (Figs 2 and 3). The reason why N116A, N116D, N116T and N116Q are active and the other 15 variants are inactive is unclear. However, there are interesting features: only the amino acid residues with side chains of moderate size can be accommodated inside the β-hairpin structure and are favourable at position 116.

In the hydrolysis of FAGLA and ZDFM, the activities were in the order N116D > WT > N116Q > N116A, N116T (Fig. 4). In the thermal treatment, the stabilities were in the order WT > N116Q > N116D, N116T, N116A (Fig. 5). These results suggest that Asn116 plays an important role in the activity and stability of thermolysin presumably by stabilizing the β-hairpin structure. It is not clear why N116D is more active than WT. Relating to this, we previously speculated the reason why thermolysin variant L144S is more active than WT: the side chain of Leu144 is buried in the interior of the protein, and thus the activation by these mutations is due to the increase in flexibility of thermolysin by the decrease in density of the inner part of the molecule (*23*). If this is true for N116D, the activation by the mutation of Asn116→Asp might be due to the increase in flexibility of thermolysin by the change in electrostatic environment of the β-hairpin structure.

It is interesting to note that N116D is more active but less stable than N116Q. This might be explained by the trade-off between activity and stability in enzymes: mutations which increase activity are accompanied with decrease in stability and vice versa (*24–26*).

The degree of the NaCl-induced activation of N116D was 11, comparable to that of WT (*15*). This suggests that that the salt-induced activation cannot be replaced by introducing mutations into Asn116. This is in contrast to our previous finding that the degree of the activations of the highly active variants, L144S and D150E, were 4 and 5, respectively, and that the salt-induced activation might be replaced to some extent (*26*).

Role of the AsnGly sequence in the β-hairpin structure in zinc-proteinases

Figure 6B shows the amino acid sequences of the β-structured polypeptides of five zinc-proteinases, *Bacillus cereus* neutral protease (*27*), *Pseudomonas aeruginosa* elastase (*28*), vibryolysin (*29*), protealysin (*30*) and human angiotensin I-converting enzyme (*31*) corresponding to Asn112–Tyr122 of thermolysin. The amino acid residues corresponding to Asn112, Ala113, Phe114, Trp115, Gly117, Ser118 and Met120 of thermolysin are highly conserved. In their crystal structures (Protein Data Bank accession

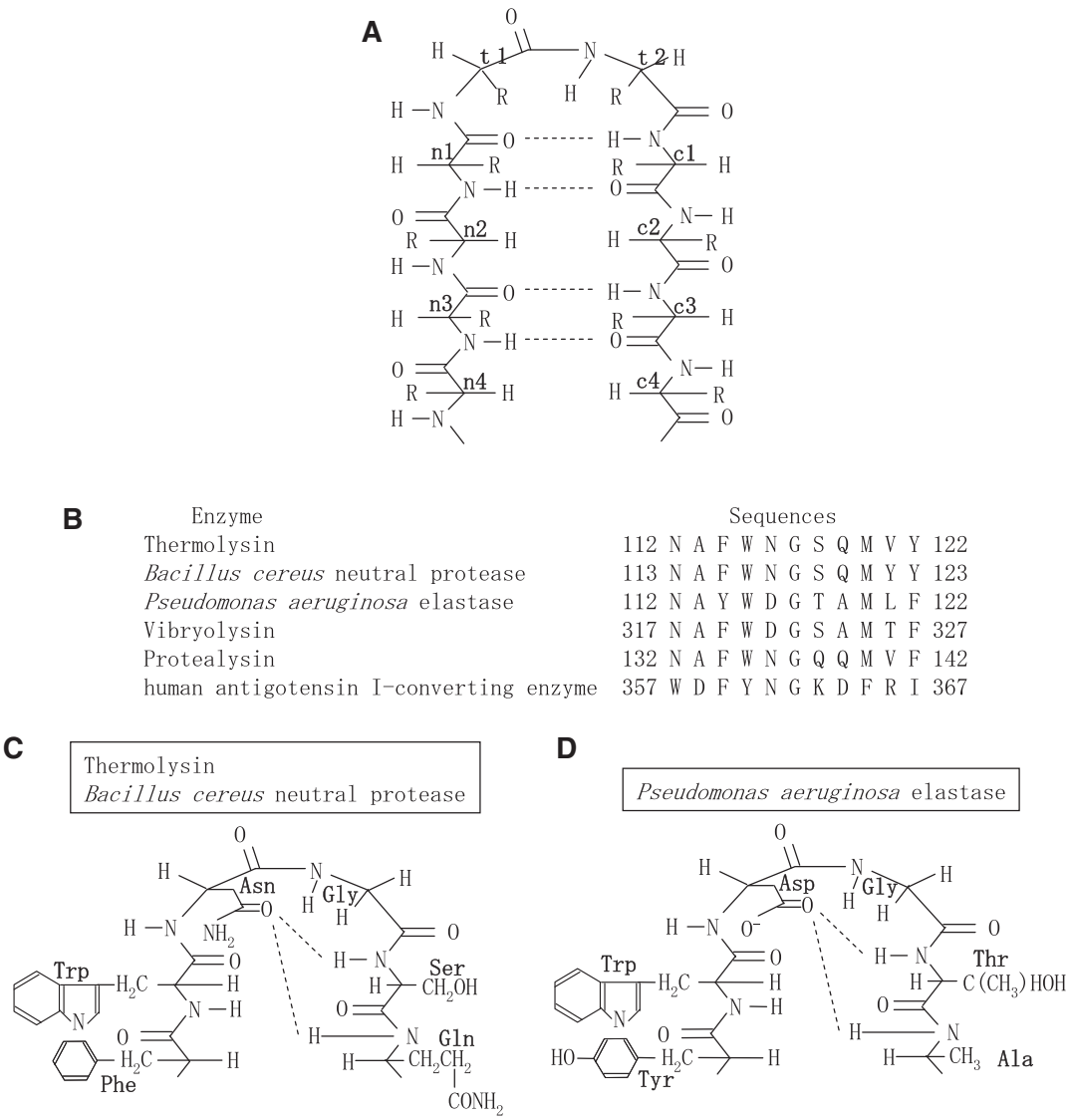

Fig. 6 β-Hairpin structure. (A) Schematic illustration of typical β-hairpin peptide backbone with two amino acid residues at the turn. Side chains are indicated by 'R'. Hydrogen bonds linking the amide hydrogen and carbonyl oxygen are indicated by dotted lines. Residues at the N-terminal β-strand, at the turn, and at the C-terminal β-strand are labelled turn as 'n', 't' and 'c', respectively. (B) Amino acid sequences of zinc-proteinases corresponding to Asn112–Tyr122 of thermolysin. (C) Schematic illustration of the β-hairpin structures of Phe114–Gln119 of thermolysin and Phe115–Gln120 of *B. cereus* neutral protease. (D) Schematic illustration of the β-hairpin structure of Tyr114–Ala119 of *P. aeruginosa* elastase.

number: *B. cereus* neutral protease, 1ESP; *P. aeruginosa* elastase, 3DBK; vibryolysin, 3NQY; protealysin, 2VQX; and human angiotensin I-converting enzyme, 1UZE), we noticed two hydrogen bonds in each of the five zinc-proteinases, corresponding to that between OD1 of Asn116 and N of Ser118 and that between OD1 of Asn 116 and N of Gln119 of thermolysin. They are the hydrogen bond between OD1 of Asn117 and N of Ser 119 and that between OD1 of Asn117 and N of Gln120 for *B. cereus* neutral protease, that between OD1 of Asp116 and N of Ser118 and that between OD1 of Asp116 and N of Ala119 for *P. aeruginosa* elastase, that between OD1 of Asp321 and N of Ser323 and that between OD1 of Asp 321 and N of Ala324 for vibryolysin, that between OD1 of Asn136 and N of Gln138 and that between OD1 of Asn136 and N of Gln139 for protealysin, and that between OD1 of Asn361 and N of Lys363 and that between OD1 of Asn361 and N of Asp364 for human angiotensin I-converting enzyme. This revealed that the AsnGly or AspGly sequence and the hydrogen bonds between the OD1 of the Asn or Asp residue at the position of i and the N of the residues at $i+1$ and $i+2$ are well conserved in zinc-proteinases.

It is thought that the carbonyl oxygen of the introduced Asp (OD1 or OD2) and Gln (OD1) forms the same hydrogen bonds as OD1 of Asn116 does. This speculation is supported by the observation that in *P. aeruginosa* elastase, the carbonyl oxygen of Asp116 forms the hydrogen bonds with the main-chain nitrogen of Thr118 and that of Ala119 (Fig. 6D). However, it should be noted that N116A has activity in spite of the fact that the introduced Ala116 does not form such hydrogen bonds. Therefore, we think that such hydrogen bonds are important, but not indispensable, for activity.

In conclusion, a highly active thermolysin variant N116D was obtained. It is suggested that Asn116 plays an important role in the activity and stability of thermolysin presumably by stabilizing the β-hairpin structure. Site-directed mutagenesis of analogous residues in the β-hairpin structure might be similarly effective in improving performances in various zinc-proteinases.

Funding
Grants-in-Aid for Scientific Research (Nos. 17380065 and 20380061) from the Japan Society for the Promotion of Science to K.I.

Conflict of interest
None declared.

References

1. Endo, S. (1962) Studies on protease produced by thermophilic bacteria. *J. Ferment. Technol.* **40**, 346–353
2. Van den Burg, B. and Eijsink, V.G. (2004) Thermolysin in *Handbook of Proteolytic Enzymes*, Vol. 1, 2nd edn. (Barrett, J.A., Rawlings, N.D., and Woessner, J.F. eds.) pp. 374–387, Elsevier, Amsterdam, The Netherlands
3. Inouye, K. (2003) Thermolysin in *Handbook of Food Enzymology* (Whitaker, J.R., Voragen, A.G.J., and Wong, D.W.S., eds.), pp. 1019–1028, Marcel Dekker, New York
4. Latt, S.A., Holmquist, B., and Vallee, B.L. (1969) Thermolysin: a zinc metalloenzyme. *Biochem. Biophys. Res. Commun.* **37**, 333–339
5. Feder, J., Garrett, L.R., and Wildi, B.S. (1971) Studies on the role of calcium in thermolysin. *Biochemistry* **10**, 4552–4556
6. Tajima, M., Urabe, I., Yutani, K., and Okada, H. (1976) Role of calcium ions in the thermostability of thermolysin and *Bacillus subtilis* var. amylosacchariticus neutral protease. *Eur. J. Biochem.* **64**, 243–247
7. Holmes, M.A. and Matthews, B.W. (1982) Structure of thermolysin refined at 1.6 Å resolution. *J. Mol. Biol.* **160**, 623–639
8. Morihara, K. and Tsuzuki, H. (1970) Thermolysin: kinetic study with oligopeptides. *Eur. J. Biochem.* **15**, 374–380
9. Inouye, K., Lee, S.-B., and Tonomura, B. (1996) Effect of amino acid residues at the cleavable site of substrates on the remarkable activation of thermolysin by salts. *Biochem. J.* **315**, 133–138
10. Inouye, K. (1992) Effects of salts on thermolysin: activation of hydrolysis and synthesis of *N*-carbobenzoxy-L-aspartyl-L-phenylalanine methyl ester, and a unique change in the absorption spectrum of thermolysin. *J. Biochem.* **112**, 335–340
11. Oyama, K., Kihara, K., and Nonaka, Y. (1981) On the mechanism of the action of thermolysin: kinetic study of the thermolysin-catalyzed condensation reaction of *N*-benzyloxycarbonyl-L-aspartic acid with L-phenylalanine methyl ester. *J. Chem. Soc., Perkin Trans. 2,* 356–360
12. Kusano, M., Yasukawa, K., and Inouye, K. (2009) Insights into the catalytic roles the polypeptide regions in the active site of thermolysin and generation of the thermolysin variants with high activity and stability. *J. Biochem.* **145**, 103–113
13. Schechter, I. and Berger, A. (1967) On the size of the active site in proteases. I. Papain. *Biochem. Biophys. Res. Commun.* **27**, 157–162
14. Menach, E., Yasukawa, K., and Inouye, K. (2010) Effects of site-directed mutagenesis of the loop residue of the N-terminal domain Gly117 of thermolysin on its catalytic activity. *Biosci. Biotechnol. Biochem.* **74**, 2457–2462
15. Yasukawa, K., Kusano, M., and Inouye, K. (2007) A new method for the extracellular production of recombinant thermolysin by co-expressing the mature sequence and pro-sequence in *Escherichia coli*. *Protein Eng. Des. Sel.* **20**, 375–383
16. Inouye, K., Minoda, M., Takita, T., Sakurama, H., Hashida, Y., Kusano, M., and Yasukawa, K. (2006) Extracellular production of recombinant thermolysin expressed in *Escherichia coli*, and its purification and enzymatic characterization. *Protein Expr. Purif.* **46**, 248–255
17. Laemmli, U.K. (1970) Cleavage of structural proteins during the assembly of the head of bacteriophage T4. *Nature* **227**, 680–685
18. Feder, J. (1968) A spectrophotometric assay for neutral protease. *Biochem. Biophys. Res. Commun.* **32**, 326–332
19. Sibanda, B.L., Blundell, T.L., and Thornton, J.M. (1989) Conformation of β-hairpins in protein structure. A systematic classification with applications to modelling by homology, electron density fitting and protein engineering. *J. Mol. Biol.* **206**, 759–777
20. Santiveri, C.M. and Jiménez, M.A. (2010) Tryptophan residues: scarce in proteins but strong stabilizers of β-hairpin peptides. *Peptide Sci.* **94**, 779–790
21. Hwang, S. and Hilty, C. (2012) Folding of a tryptophan zipper peptide investigated on the basis of the nuclear Overhauser effect and thermal denaturation *J. Phys. Chem. B* **115**, 15355–15361
22. Wu, L., McElheny, D., Setnicka, V., Hilario, J., and Keiderling, T.A. (2012) Role of different β-turns in β-hairpin conformation and stability studies by optical spectroscopy. *Proteins* **80**, 44–60
23. Yasukawa, K. and Inouye, K. (2007) Improving the activity and stability of thermolysin by site-directed mutagenesis. *Biochim. Biophys. Acta* **1774**, 1281–1288
24. Shoichet, B.K., Baase, W.A., Kuroki, R., and Matthews, B.W. (1995) A relationship between protein stability and protein function. *Proc. Natl Acad. Sci. USA* **92**, 452–456
25. Lee, S., Oneda, H., Minoda, M., Tanaka, A., and Inouye, K. (2006) Comparison of starch hydrolysis activity and thermal stability of two *Bacillus licheniformis* α-amylase and insights into engineering α-amylase variants active under acidic conditions. *J. Biochem.* **139**, 997–1005
26. Kusano, M., Yasukawa, K., and Inouye, K. (2010) Effects of the mutational combinations on the activity and stability of thermolysin. *J. Biotechnol.* **147**, 7–16
27. Lister, S.A., Wetmore, D.R., Roche, R.S., and Codding, P.W. (1996) E144S active-site mutant of the *Bacillus cereus* thermolysin-like neutral protease at 2.8 Å resolution. *Acta Crystallogr. D Biol. Crystallogr.* **52**, 543–550
28. Thayer, M.M., Flaherty, K.M., and KcKay, D.B. (1991) Three-dimensional structure of the elastase of *Pseudomonas aeruginosa* at 1.5-Å resolution. *J. Biol. Chem.* **266**, 2864–2871

29. Gao, X., Wang, J., Yu, D.Q., Bian, F., Xie, B.B., Chen, X.L., Zhou, B.C., Lai, L.H., Wang, Z.X., Wu, J.W., and Zhang, Y.Z. (2010) Structural basis for the autoprocessing of zinc metalloproteases in the thermolysin family. *Proc. Natl Acad. Sci. USA* **107**, 17569–17574
30. Demidyuk, I.V., Gromova, T.Y., Polyakov, K.M., Melik-Adamyan, W.R., Kuranova, I.P., and Kostrov, S.V. (2010) Crystal structure of the protealysin precursor: insights into propeptide function *J. Biol. Chem.* **285**, 2003–2013
31. Natesh, R., Schwager, S.L., Sturrock, E.D., and Acharya, K.R. (2003) Crystal structure of the human angiotensin-converting enzyme-lisinopril complex. *Nature* **421**, 551–554